Interpretation of polarimetric ice penetrating radar data over Antarctic ice shelves.

C S M Doake, H F J Corr, A Jenkins, K W Nicholls and C Stewart
British Antarctic Survey, Natural Environment Research Council, Madingley Road, Cambridge, CB3 0ET, UK

Abstract

We have collected ice penetrating polarimetric radar data on Brunt, George VI and Ronne ice shelves using a vector network analyser as a continuous wave (CW) step-frequency radar. Being a wideband phase sensitive instrument, the radar allowed the vectorial nature of the interaction between radio waves and the ice and reflecting surface to be explored. Single crystals of ice are birefringent not only at optical frequencies but also at radar ones, so in an ice sheet the average crystal orientation fabric determines the overall level of birefringence. The polarisation of radio waves is changed by the birefringent nature of the ice and by the reflecting surface, whether an internal layer or the basal boundary. By transmitting and receiving on orthogonal linearly polarised aerials, we could use a scattering matrix approach to determine the parameters describing the action of the ice and reflecting surface on the polarisation behaviour.

Introduction

The depolarisation behaviour of ice sheets on radar waves transmitted through them and reflected from the base or from internal horizons has been recognised since the early days of radio-echo sounding in the 1960s (Jiracek 1967). Several studies have been made of the phenomenon but the relatively unsophisticated equipment in use until recently meant that only power could be measured, not phase (Bogorodskiy et al, 1970; Kluga et al, 1973; Clough, 1974; Bentley, 1975; Woodruff and Doake, 1979; Yoshida et al, 1987; Fujita and Mae, 1993). Extracting relevant physical parameters required aerials to be rotated to gather sufficient measurements. Hargreaves (1977, 1978) rotated crossed dipoles and obtained reflections from internal layers in Greenland. He interpreted his results in terms of an overall birefringence of the ice and established the relationship between a crystal orientation fabric and the birefringence. Woodruff and Doake (1979) rotated separate transmitting and receiving dipoles over Bach Ice Shelf in the Antarctic Peninsula.

By measuring phase as well as amplitude, it is possible to construct a polarimetric radar that requires only orthogonal aerials, making it suitable for airborne use. It is possible to simulate from measurements on orthogonal linearly polarised aerials the observations that would have been made at any other polarisation state, for example different orientations of linearly polarised aerials or even circularly polarised ones.

Polarimetric radars have been flown on aircraft (e.g. AirSAR, CARABAS, E-SAR, SASAR, etc) and satellites (e.g. ERS1/2, RADARSAT, etc) for studying the earth's surface. They tend to be associated with synthetic aperture radars (SAR) and operate at frequencies too high for significant penetration into ice sheets, although P-band (~450 MHz) or VHF (~140 MHz) SARs might be successful if flown at suitable altitudes. There are also ground based polarimetric systems for investigating small regions. Polarimetric information is normally used to help discriminate targets in SAR images rather than infer physical properties of the target surfaces.

Early attempts with a ground based radar to produce SAR images of glacier beds were time consuming (Musil, 1987, 1989; Musil and Doake, 1987) and covered only a very small area, so the technique was not pursued. With modern radar equipment there seems no real impediment to achieving our goal of imaging the bed of a glacier. This ability would revolutionise the interpretation of basal conditions on ice sheets, ice streams and ice shelves. However, ground based systems would have limited areal coverage and airborne systems would require lower operating frequencies than normally used for airborne SARs. In either case there is the problem of correcting the distortion caused by birefringence in the ice. Polarimetric information is needed to sharpen SAR images.

Both the ice and reflecting surfaces are of interest, the ice sheet because of the crystal fabric responsible for the birefringence, which in turn is a product of the strain/stress history of the ice sheet, and the reflecting surfaces for the insight they can give into internal processes and the nature and conditions of the basal zone.

In this paper, we concentrate on describing the polarisation behaviour of radio waves propagating through and reflected within and at the base of ice sheets. Ground based radar data are analysed using a scattering matrix approach to determine physical properties of both the ice and the reflecting surfaces.

Propagation of electromagnetic waves in ice

Single crystals of naturally occurring ice Ih have hexagonal symmetry (space group symbol $P6_3$/mmc, number 194; Laue class symmetry 6/mmm), which allows for birefringence but not optical activity (Hargreaves, 1977). The permittivity of a birefringent material can be represented by a real symmetric tensor with two of the three principal values identical; the difference between the two principal values is the birefringence. The principal axis of rotational symmetry is called the optic axis and the medium is called uniaxial. Ice is therefore classed as a uniaxial birefringent medium. In ice, the optic axis coincides with the crystallographic c-axis.

We make the assumption that a polycrystalline ice sheet also exhibits a birefringent behaviour, with a strength determined by the crystal orientation fabric (Hargreaves, 1978). Plane wave solutions of Maxwell's equations show that only two directions are allowed for propagation, the extraordinary wave in the plane containing the optic axis and the ordinary wave in the plane perpendicular to it (Hargreaves, 1978). Ice is optically positive, so that the velocity of the ordinary ray is greater than the extraordinary ray. The propagation vectors are different in the two directions, leading to a change in phase between the field components such that an incident wave that is linearly polarised will become elliptically polarised after passing through the medium.

Sinclair scattering matrix

Backscatter convention

Coherent backscatter of completely polarised plane electromagnetic waves from deterministic targets is described by a 2x2 complex scattering matrix called the Sinclair matrix (Lüneburg, 2002), which is the analogue of the Jones matrix in optical or forward scattering (i.e. transmission) situations. In the 'Back Scatter Alignment' (BSA) convention (Ulaby and Elachi, 1990), which uses a common 2-dimensional orthonormal polarization basis for the transmitted and received waves, the Sinclair matrix is symmetric for reciprocal targets. Much confusion exists in the radar literature because of incorrect interpretations of backscatter data in terms of optical transmission theory, which is usually described using the 'Forward Scattering Alignment' (FSA) convention (Ulaby and Elachi, 1990; Lüneburg, 2002). Using the FSA convention for backscatter means that the domain and range of the scattering matrix (Horn and Johnson, 1985; p5) do not belong to the same propagation space and they also refer to different coordinate systems. These drawbacks prevent, for example, the straightforward application of eigenvector analysis for finding the polarisation invariants (Lüneburg, 2002). A solution is the use of the 'time reversal' concept, as formulated first for quantum mechanical systems, and the associated complex conjugation operation. An outline of the derivation of the basic equations of radar polarimetry in the BSA convention is given in the rest of this sub-section.

Let $\mathbf{E}(z)$ be a complex vector describing a plane harmonic electromagnetic wave travelling in the z direction. In a Cartesian coordinate frame (x, y) transverse to z, the total electric field vector $\mathbf{E}$ is given by

$$\mathbf{E} = E_x\,\mathbf{x} + E_y\,\mathbf{y},$$

with the field components given by

$$E_x = E_{x0} \exp i(\omega t - kz)$$
$$E_y = E_{y0} \exp i(\omega t - kz + \delta)$$

where ω is the angular frequency, t is time, k is the wavenumber, δ is the phase difference between components, E_{x0}, E_{y0} are the amplitudes of the components and $\mathbf{x}$, $\mathbf{y}$ are unit vectors in the x, y directions respectively. The column vector $\mathbf{E} = [E_x, E_y] = [E_{x0}, E_{y0} \exp(i\delta)]$, where the common factor $\exp i(\omega t - kz)$ has been removed, is called the Jones vector.

The polarisation of a wave travelling in a direction specified by the propagation vector $\mathbf{z}$ is defined as the locus of the polarisation ellipse and the sense of rotation of the electric field vector with respect to $\mathbf{z}$, i.e. the handedness. The locus is a geometrical quantity which can be represented by a complex Jones vector once a particular basis has been established. However, although the rotation can be determined from the Jones vector by the relative phase difference δ between the two components, the handedness cannot. Changing the direction from $\mathbf{z}$ to $-\mathbf{z}$ implies a change in handedness and in the sign of δ, or equivalently, a transition to the complex conjugate of the Jones vector.

In the monostatic radar case, by introducing at the aerial a common Cartesian coordinate system **B**={**e**$_1$, **e**$_2$} for the domain and range (Horn and Johnson, 1985; p5) of the scattering matrix, S_M, the backward scattering process can be described by the field equation for radar polarimetry (Lüneburg, 2002)

$$\mathbf{E}^{\mathbf{s}} = S_M\,\mathbf{E}^{\mathbf{i}} \qquad (1)$$

where the superscripts s and i denote scattering and incidence. The basis vectors $\mathbf{e}_i$ (i = 1, 2) are associated with the unit coordinate vectors **x** and **y,** or with any other linear orthonormal polarisation basis transverse to **z**. Then, the polarisation of a wave travelling in the + (forward/transmit) direction,

$$\mathbf{E}^+ = E_1^+\,\mathbf{e}_1 + E_2^+\,\mathbf{e}_2$$

has the same polarisation as a wave travelling in the opposite (-/receive) direction

$$\mathbf{E}^- = E_1^-\,\mathbf{e}_1 + E_2^-\,\mathbf{e}_2$$

if $E_1^- = E_1^{+*}$ and $E_2^- = E_2^{+*}$ where the superscript * denotes complex conjugation. Using this nomenclature, the radar polarimetry equation becomes, (Lüneburg, 2002),

$$\mathbf{E}^{\mathbf{s-}} = S_M\,\mathbf{E}^{\mathbf{i+}} = S_M\,\mathbf{E}^{i-*}$$

where the symmetric Sinclair scattering matrix is given by

$$S_M = S_M^T = \begin{bmatrix} s_{11} & s_x \\ s_x & s_{22} \end{bmatrix} \qquad s_x = s_{12} = s_{21}\ .$$

The Sinclair matrix S_M links the forward travelling wave with the backscattered one, in the same 2-dimensional coordinate system **B** orthogonal to the direction of travel. The opposite directions of travel for the incident and scattered wave are best linked by the concept of time reversal, which implies conjugation. This unifies the underlying space for the forward and backward scattering. Mathematically, this requires the definition of an antilinear operator T_a such that

$$\mathbf{E}^{s+} = T_a(\mathbf{E}^{i+})$$

where the + subscript denotes travel in the forward (transmission) direction. The action of the operator is to take the complex conjugate of its argument and multiply it be a matrix, the so-called matrix part of the antilinear operator. Thus, the Sinclair matrix S_M is the matrix part of the antilinear backscatter operator T_a (Lüneburg and Cloude, 1997b).

In physical optics, an eigenmode analysis of the scattering matrix gives the two (complex) eigenvectors corresponding to the two orthogonal polarisation states which are transmitted and received at the same polarisation state, while the eigenvalues are the corresponding (complex) amplitudes of these two states. A similar relationship exists for radar polarimetry, where however, the polarisation invariants are determined from the coneigenvector equation (Horn and Johnson, 1985, p245), known in the radar community as Kennaugh's pseudo-eigenvalue equation (Lüneburg, 2002),

$$S_M \mathbf{x} = \lambda \mathbf{x}^* \tag{2}$$

where $\mathbf{x}^*$ is the complex conjugate of the coneigenvector $\mathbf{x}$ and λ is a coneigenvector of S_M. Equation (2) is the basic equation of radar polarimetry (Lüneburg and Boerner, 1997).

Polarisation signatures

Knowing the scattering matrix S_M allows the power that would be received for any combination of transmit and receive polarisations to be calculated. Two particular cases are commonly considered, one where the transmit and receive polarisations are the same, called the co-polarised signature, P_{co}, and the other for orthogonal polarisations, called the cross-polarised signature, P_x:

$$P_{co} = p^T S_M p;$$

$$P_x = p^T S_M p_x$$

where p is the polarisation state, described for example by the orientation and ellipticity of the polarisation ellipse, p^T is the transpose of p, and p_x is the orthogonal polarisation. Polarisation signatures (or polarisation responses) are a plot of the synthesised scattering cross section as a function of the orientation and ellipticity of the transmitted wave. They give a qualitative means of describing the polarisation effects of the transmission medium (in this case ice) and the target reflecting surface (Ulaby and Elachi, 1990).

Ice sheet representation

For near-vertical propagation through an ice sheet, we assume that a (monochromatic) wave has its electric field components in the x and y directions of a rectangular coordinate system based in the near-horizontal surface (Figure 1). The near-vertical plane containing the effective optic axis is taken to define the y direction (Hargreaves, 1977), whose bearing is initially unknown and is one of the parameters to be determined. The rectangular coordinate system (x', y') in which the measurements are made is orientated at an angle ε to the x-axis. The ice sheet is modelled as a birefringent medium characterised by a two-way phase shift, δ, and orientation of the effective optic axis, ε. Reflection from a rough surface at near-normal incidence is described by different reflection coefficients along orthogonal axes oriented at an angle γ to the optic axis ((S,S) in Figure 1). Although each Fresnel reflection coefficient will in general be complex, the effect on the polarisation behaviour will be given by their ratio, r (taken so that $r \geq 1$) which is assumed to be real. Backscatter of a fully polarised wave, transmitted on a linearly polarised aerial at an angle β to the x-axis and received on a linearly polarised aerial at an angle θ to the x-axis, can be described by (Doake, 1981):

$$E_R(\theta) = R(\theta)\, P(\delta/2)\, R(\gamma)\, S(r)\, R(-\gamma)\, P(\delta/2) R(-\beta)\, E_T \tag{3}$$

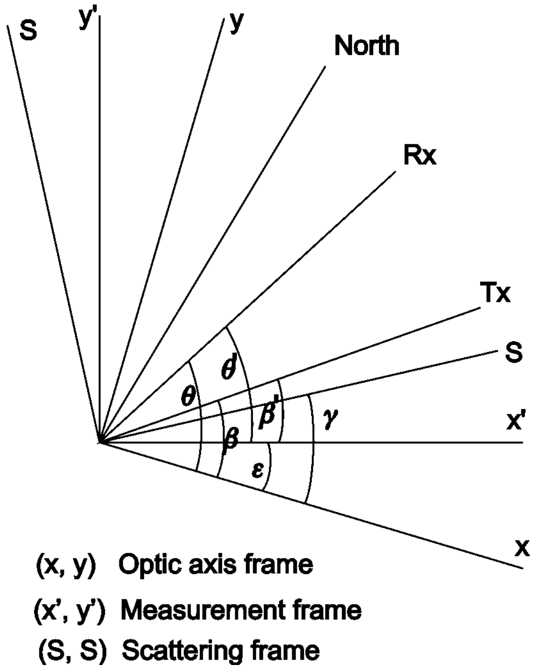

Figure 1. *Relationship between coordinate systems for field measurements, reflecting surface and optic axis. Tx is the orientation of transmitting aerial, Rx the orientation of the receiving aerial.*

where

$E_R = [E_{r1}\ ,\ 0]^T$ and $E_T = [E_{t1}\ , 0]^T$ in their respective aerial coordinate systems and

$$P(\delta) = \begin{bmatrix} 1 & 0 \\ 0 & \exp(i\delta) \end{bmatrix},\quad S(r) = \begin{bmatrix} 1 & 0 \\ 0 & r \end{bmatrix},\quad R(\theta) = \begin{bmatrix} \cos\theta & \sin\theta \\ -\sin\theta & \cos\theta \end{bmatrix}.$$

Here, P is the phase shift matrix, S the target scattering matrix and R the rotation matrix.

In polarimetry it is conventional to refer to orthogonally polarised wave directions as H (horizontal) and V (vertical), where for oblique incidence of a wave onto a scattering surface these directions bear some obvious relation to the directions of the transmitted E vector. Although for the near normal incidence used in glacier sounding there is no real distinction between H and V, we shall use the convention as a convenient means of distinguishing between waves transmitted along the x'-axis (H) and the y'-axis (V). For transmitting and receiving on orthogonal (e.g. linearly) polarised aerials where H is orientated at an angle ε to the x-axis, equation (3) can be written as

$$E_R = R(\varepsilon)\ P(\delta/2)\ R(\gamma)\ S(r)\ R(-\gamma)\ P(\delta/2)\ R(-\varepsilon)\ E_T \qquad (4)$$

where for brevity we write

E_R = [H, V]^T, E_T = [H, V]^T with the understanding that only one of the H or V components is implied in any single measurement with the stated aerial system.

Decomposition of Sinclair matrix

Comparison of equations (1) and (4) shows that the Sinclair matrix is given by

$$S_M = \begin{bmatrix} HH & HV \\ VH & VV \end{bmatrix} = R(\varepsilon)P(\delta/2)R(\gamma)S(r)R(-\gamma)P(\delta/2)R(-\varepsilon) \ . \qquad (5)$$

It is assumed, by Lorentz' theorem of reciprocity, that HV=VH, so S_M is symmetric. There are therefore six independent parameters that can be determined from the three complex elements of S_M.

For a three parameter model, where the ice sheet is described by two parameters, an optical axis direction ε and a phase shift δ, and the reflecting surface by a single parameter, r, the ratio of reflection coefficients in the two orthogonal directions parallel and perpendicular to the optic axis, all three can be found directly from a (con)eigenmode analysis. However, we find that three parameters are insufficient to fit the measurements and another one is required. There are cross-polarisation terms which can be accounted for by allowing the principal axes of the reflecting surface to be oriented at an angle γ to the optic axis. While this modification is not the only way of introducing the cross-polarised terms (for example, it is mathematically equivalent to having non-zero off-diagonal terms in the (symmetric) target scattering matrix S) it has the advantage of having a simple physical interpretation which can be easily visualised and related to real surfaces.

Instead of a (con)eigenmode analysis, an iterative/analytical method has been used to decompose the scattering matrix S_M into its constituent matrices to give the values of the 4 parameters (γ, ε, r, δ). An 'absolute' amplitude and phase (R, f) can also be calculated, which can be considered as a normalising factor for the scattering matrix.

There is also a set of 'complementary' solutions ($\pm\pi/2-\gamma$, $\varepsilon \pm\pi/2$, r, 2π-δ) whose polarisation signature has the same amplitude pattern but differs in phase by the amount, δ. The matrix S_{MC} formed by using the complementary values in equation (5) above for S_M:

$$S_{MC} = R(\varepsilon+\pi/2)\, P(\pi-\delta/2)\, R(\pi/2-\gamma)\, S(r)\, R(-\pi/2+\gamma)\, P(\pi-\delta/2)\, R(-\varepsilon-\pi/2)$$

is related to S_M by

$$S_M = S_{MC} \exp(i\ \delta).$$

The need for complementary solutions is revealed when field data is analysed. When calculating parameter values over a continuous range of depths, the iterative/analytic solution method produces sudden jumps in the values of the parameters γ, ε, and δ. However, if the complementary solutions are calculated as well, the jumps are shown to be transitions between double-valued parameters (Figure 2). The value of r is single valued, as reciprocal values of r do not affect the solution procedure. In a forward model, but not with real data, it is possible to distinguish between the 'real' and 'complementary' solutions.

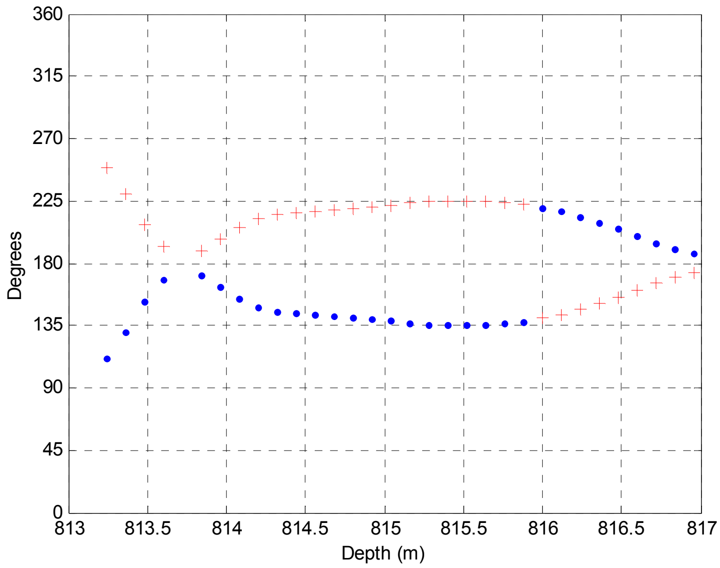

Figure 2. *Plot of phase shift introduced in two-way path through the ice. There are two solutions to the scattering matrix, δ (dots) and 2π-δ (crosses), both of which are needed to give a continuous variation of phase with depth.*

Supplementary scattering matrix

The matrix given by

$$S_S = \begin{bmatrix} HH & -HV \\ -VH & VV \end{bmatrix} = R(-\varepsilon)P(\delta/2)R(-\gamma)S(r)R(\gamma)P(\delta/2)R(\varepsilon)$$

has solutions ($-\gamma$, $-\varepsilon$, r, δ), closely tied to those from the Sinclair matrix and again with a complementary set, ($\gamma+\pi/2$, $\pi/2-\varepsilon$, r, 2π-δ), which form the complementary supplementary-Sinclair matrix S_{SC} (Table 1). As with the principal Sinclair matrix, the relationship between S_S and S_{SC} is given by

$$S_S = S_{SC}\exp(\mathrm{i}\,\delta)\ .$$

The origin of, and solutions to, the supplementary-Sinclair matrix can be described in a coordinate frame in which angles are regarded positive in the opposite sense to the Sinclair matrix – i.e. clockwise instead of anti-clockwise. The polarisation signatures for S_M and S_S are similar, but rotated through 180 degrees.

Table 1: Relationship between values of polarisation parameters

	Orientation of reflection axes	Orientation of optic axis	Ratio of reflection coefficients	Phase difference
S_M	γ	ε	r	δ
S_{MC}	$\pm\pi/2-\gamma$	$\varepsilon\pm\pi/2$	r	2π-δ
S_S	$-\gamma$	$-\varepsilon$	r	δ
S_{SC}	$\pm\pi/2+\gamma$	$-\varepsilon\pm\pi/2$	r	2π-δ

Aerial calibration

The supplementary matrix arises because of the two different senses for rotating the orthogonal aerials to their measurement positions. If a pair of linearly polarised aerials is used for transmitting and receiving, then rotating the 'horizontal' aerials anti-clockwise to form the 'vertical' direction will give the Sinclair matrix, S_M. If, however, the sense of rotation is clockwise the data gathered will give the supplementary Sinclair matrix, S_S. Knowing the sense of rotation, the appropriate sign can be assigned to the data and consistent results obtained. To avoid ambiguity when a fixed set of aerials is used, for example a pair of crossed dipoles, or fixed dipoles on an aircraft, where no rotation is involved in the measurement procedure, it is essential that the aerial system is calibrated to ensure that the correct sense is chosen when analysing the data.

Coneigenmode analysis

Complementary solutions may be connected with the fact that equation (2) always has two orthogonal solutions for **x** if the scattering matrix is symmetric (Lüneburg and Cloude, 1997a). We solve equation (2) by writing it in the form (Horn and Johnson, 1985, p245),

$$(S_M S_M^*)\,\mathbf{x} = |\lambda|^2\,\mathbf{x}$$

where S_M^* is the component-wise conjugate of S_M, which shows that the (positive) square roots of the eigenvalues of $S_M S_M^*$ are the coneigenvalues of S_M and the eigenvectors of $S_M S_M^*$ are the coneigenvectors of S_M. The form of the equation shows that for arbitrary φ the matrix $S_M \exp(i\varphi)$ will have the same coneigenvectors and coneigenvalues as S_M. There is also an inherent phase indeterminacy of the coneigenvalues arising from the nature of equation (2) (Lüneburg, 2002). If **x** is a solution and λ is a coneigenvalue of S_M then $\lambda e^{2i\varphi}$ is also a coneigenvalue since, for arbitrary φ,

$$S_M\,(e^{i\varphi}\mathbf{x}) = e^{2i\varphi}\lambda\,(e^{i\varphi}\,\mathbf{x})^*\,.$$

Not only are there an infinite number of coneigenvalues for a given (symmetric) matrix, there are an infinite number of (symmetric) matrices with the same coneigenvectors. This contrasts with ordinary eigenvalue equations, which have only finitely many distinct eigenvalues (Horn and Johnson, 1985, p245). Interpretation and significance of the phase indeterminacy is not fully understood (Lüneburg, 2002).

Thus, the coneigenvectors of S_M and S_{MC} are identical, as are those for S_S and S_{SC} . We find that the coneigenvectors of S_M and S_S are Hermitian adjoints (Horn and Johnson, 1985, p6) of each other. The coneigenvalues of S_M, S_{MC}, S_S and S_{SC} are identical (positive, real) and give the value of r directly.

Writing S_M from equation (5) in the form

$$S_M = R(\varepsilon)\,K\,R(-\varepsilon) = R\,K\,R^{-1}$$

where $K = P(\delta)\, R(\gamma)\, S(r)\, R(-\gamma)\, P(\delta)$ shows that the kernel K of the scattering matrix is (con)similar with S_M and has the same (con)eigenvalues.

Distortion matrices

Errors in the scattering matrix can be caused by imperfections in the transmitting and receiving aerials. It is common to use aerial distortion matrices to model these errors. The measured scattering matrix M can be represented in terms of the actual scattering matrix S_M and distortion matrices D_r for the receive aerial and D_t for the transmit aerial:

$$M = D_r\, S_M\, D_t\ .$$

We have not applied any corrections to our measured scattering matrices.

Data collection and analysis

A vector network analyser (HP8751A) was used as a step-frequency radar, transmitting a series of increasing tones (fixed frequencies with constant separation, Δf), each for a set length of time (Figure 3). For glacier sounding, the separation between tones is adjusted according to the expected ice thickness (maximum range is proportional to 1/Δf), while the number of tones multiplied by their separation gives the bandwidth. Thus, thicker ice implies reduced available bandwidth for a given number of tones. The length of time for which each tone is transmitted (called the i.f. bandwidth) determines the noise level; longer transmissions give lower noise, but increase the measurement time. Fourier techniques transform the signal to its equivalent pulse in the time domain.

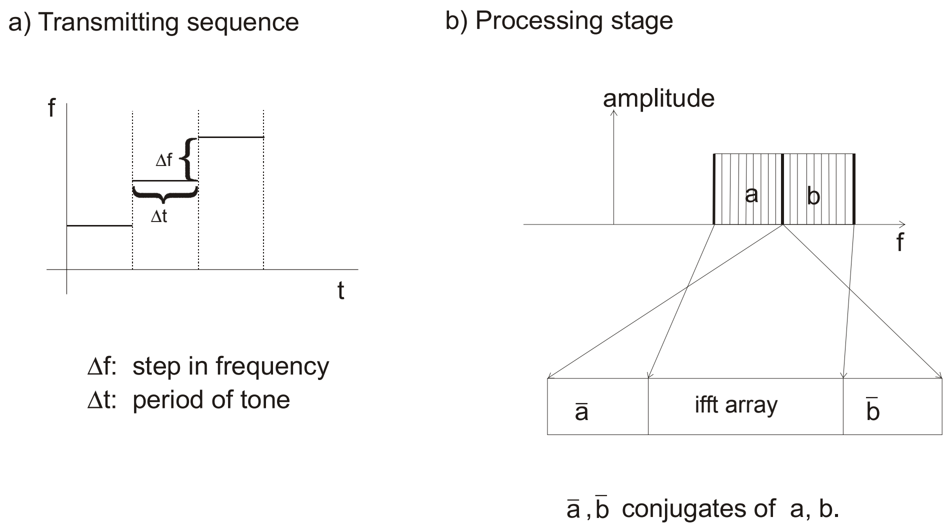

Figure 3. *Step frequency radar. (a) A series of discrete frequencies are transmitted. The ice depth and the required noise level determine the number and duration of the tones and the frequency interval between them. (b) The amplitude and phase of each frequency component are transposed into an array that is processed by an inverse Fourier transform. The data points to be processed can be selected to simulate different centre frequencies and bandwidths. The bandwidth and size of the ifft array determine the depth resolution of the parameters.*

Usually a bandwidth of up to about 200 MHz was used, with transmit frequencies ranging from around 200 to 400 MHz. When processing the data, both the bandwidth and centre frequency can be adjusted. Thus we can either select the full bandwidth, which gives the highest depth resolution, or we can narrow the bandwidth and simulate the effect of moving a window across the full frequency range. This allows the frequency dependence of the scattering matrix parameters to be measured and also simulates the response of airborne radar systems, which have rather narrow bandwidths compared with the network analyser. Smaller bandwidths give less depth resolution, acting as a smoothing filter on the derived polarisation parameters.

Frequency dependence of the birefringence

The relationship between the observed phase shift δ and the birefringence $\Delta\varepsilon$ is given by (Doake, 1981)

$$\delta = (2\pi/\lambda)(n_e - n_o)2H = (2\pi/\lambda)\Delta n 2H = 2\pi H n b f/c$$

which can be recast as

$$b = \delta c/(2\pi H n f) = \delta\lambda/(2\pi H n) \qquad (6)$$

where δ = phase shift measured in scattering matrix decomposition (i.e. two-way travel through the ice), H is thickness of layer, ε is the permittivity of ice, b the relative birefringence (= $\Delta\varepsilon/\varepsilon \approx 2\Delta n/n$), n the refractive index ($=\sqrt{\varepsilon}$), f the frequency of the radio waves, λ their wavelength and c the velocity of electro-magnetic waves in vacuo.

When decomposing the Sinclair matrix at a single frequency, we can only determine δ modulo 2π. However, we can take advantage of the frequency dependence of the birefringence and the wide bandwidth of the radar to resolve this 2π ambiguity and give a more accurate lower bound to the birefringence. For a given depth, the values of the optic axis direction γ and phase shift δ were calculated for different centre frequencies covering the range of the original data. We modelled the observed behaviour by a two-layer ice sheet, with each layer having a different optic axis orientation and birefringence. The model parameters were adjusted to give a close fit to the observations, without a formal optimisation procedure being used (Figure 4).

Results and discussion

Only very preliminary results are given here, to illustrate some of the principles discussed above. We took representative sites from Rutford Ice Stream grounding zone, Korff Ice Rise and the north-west corner of Ronne Ice Shelf, and analysed the radar data using a two-layer model for the frequency dependence of the orientation of the optic axis and the phase difference, δ. Using equation (6) gives values of birefringence shown in Table 2. The greatest value of 0.15% is well below the value of 1.1% given for the birefringence of a single ice crystal (Matsuoka et al, 1997), suggesting that the ice fabric is rather weak and not particularly anisotropic.

There is a clear distinction between the upstream sites (Rutford and Korff) where the birefringence is around the 0.1% level and the site near the ice front (NW Ronne)

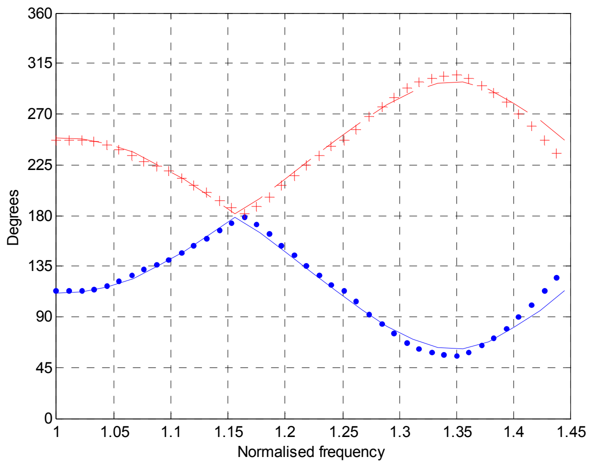

.

Figure 4. *Plot of frequency dependence of phase shift introduced in two-way path through the ice. Principal values are shown by dots (measured) and continuous line (modelled); complementary values are shown by crosses (measured) and dashed line (modelled). Model parameters: top layer, phase shift 215 degrees; bottom layer, phase shift 840 degrees.*

where it is about half that value. This can be understood if the lower layer of ice, with the strongest birefringence, is melting off into the sea and being replaced by randomly oriented snow crystals with a weaker fabric on the surface.

Table 2: Polarisation parameters.

	Optic axis bearing		Phase shift		Thickness	Initial frequency	Relative birefringence
	ε_1	ε_2	δ_1	δ_2	H (m)	f_0 (MHz)	b (%)
Rutford	-40	30	50?	1400?	1570	273	.09?
Korff	-45	30	215	840	816	230	.15
NW Ronne	90	-40	50	110	399	230	.05

Propagation delay times

When the radar data are displayed in the time domain, the equivalent pulse reflected from the base or an internal layer can be readily identified. Different orientations of the aerial give a small spread of arrival times. This spread is related to the birefringence, as the ordinary and extraordinary wave will travel at slightly different speeds. The relationship $b = \Delta\varepsilon/\varepsilon \approx 2\Delta n/n$ shows that a 0.1% level of birefringence will give a 1 m difference in apparent depth in ice 2000 m thick.

Ice sheet modelling

Fabric evolution can be included in an ice sheet model to predict the birefringence, which can be checked by field measurement. Such modelling work will also have to include realistic reflecting characteristics for basal and internal layers. Even if the polarisation parameters are not reproduced precisely, their variation and pattern of change with position over an area can be compared.

Conclusions

The vector network analyser used as a polarimeter is a very powerful instrument for investigating the structure and properties of ice sheets and their reflecting horizons, both basal and internal. A scattering matrix approach to collecting and analysing data is flexible enough to be used on an airborne system, opening up the possibility of developing an airborne SAR capable of imaging the subglacial environment, such as glacier beds and ice shelf bottoms.

References

Bentley, C.R. 1975. Advances in geophysical exploration of ice sheets and glaciers. *Journal of Glaciology*, 15(73), 113-135.

Bogorodskiy, V.V., Trepov, G.V. and Fedorov, B.A. 1970. On measuring dielectric properties of glaciers in the field. (*In* Gudmandsen, P., ed. *Proceedings of the international meeting on radioglaciology, Lyngby, May 1970*. Lyngby, Technical University of Denmark, Laboratory of Electromagnetic Theory, 20-31.)

Clough , J.W. 1974. *Propagation of radio waves in the Antarctic Ice Sheet*. Ph.D thesis, University of Wisconsin.

Doake, C.S.M.1981. Polarization of radio waves in ice sheets. *Geophysical Journal of the Royal astronomical Society*, 64, 539-558.

Fujita, S. and Mae, S. 1993. Relation between ice sheet internal radio-echo reflections and ice fabric at Mizuho Station, Antarctica. *Annals of Glaciology*, 17, 269-75.

Hargreaves, N.D. 1977. The polarization of radio signals in the radio echo sounding of ice sheets. *Journal of Physics. D Applied Physics*, 10(9), 1285-1304.

Hargreaves, N.D.1978. The radio frequency birefringence of polar ice. *Journal of Glaciology*, 21, 301-313.

Horn, R.A. and Johnson, C.R. 1985. *Matrix analysis*. Cambridge University Press, pp561.

Jiracek, G.R.1967. Radio sounding of Antarctic ice. *University of Wisconsin Geophysical and Polar Research Centre, Research Report Series No. 67*, 1-127.

Kluga, A.M., Trepov, G.V., Fedorov, B.A. and Khokhlov, G.P. 1973. Some results of radio-echo sounding of Antarctic glaciers in the summer of 1970-71. *Trudy Sovetskoy Antarkticheskoy Ekspeditsii*, Tom 61, 151-63.

Lüneburg, E. 2002. Aspects of radar polarimetry. *Turkish Journal of Electrical Engineering and Computer Sciences*, 10(2), 219-243.

Lüneburg, E. and Boerner, W.-M. 1997 Homogeneous and inhomogeneous Sinclair and Jones matrices. *In* Mott, H. and Boerner, W-M, Eds, *Wideband interferometric sensing and imaging polarimetry, Proceedings of SPIE (The International Society for Optical Engineering)*, Vol 3120, 45-54.

Lüneburg, E. and Cloude, S.R. 1997a. Bistatic scattering. *In* Mott, H. and Boerner, W-M, Eds, *Wideband interferometric sensing and imaging polarimetry, Proceedings of SPIE (The International Society for Optical Engineering)*, Vol 3120, 56-68.

Lüneburg, E. and Cloude, S.R. 1997b. Radar versus optical polarimetry. *In* Mott, H. and Boerner, W-M, Eds, *Wideband interferometric sensing and imaging polarimetry, Proceedings of SPIE (The International Society for Optical Engineering)*, Vol 3120, 361-372.

Matsuoka, T., Fujita, S., Morishima, S. and Mae, S. 1997. Precise measurement of dielectric anisotropy in ice Ih at 39 GHz. *Journal of Applied Physics*, 81(5), 2344-48.

Musil, G.J. 1987. *Synthetic aperture radar sounding through ice*. M.Sc. thesis, University of Cambridge.

Musil, G.J. and Doake C.S.M. 1987. Imaging subglacial topography by a synthetic aperture radar technique. *Annals of Glaciology*, 9, 170-175.

Musil, G.J. 1989. On the underside scarring of floating ice sheets. *Annals of Glaciology*, 12, 118-123.

Woodruff, A.H.W. and Doake, C.S.M. 1979. Depolarisation of radio waves can distinguish between floating and grounded ice sheets. *Journal of Glaciology*, 23(89), 223-232.

Yoshida, M., Yamashita, K. and Mae, S. 1987. Bottom topography and internal layers in East Dronning Maud Land, East Antarctica, from 179 MHz radio echo-sounding. *Annals of Glaciology*, 9, 221-224.

Ulaby, F.T. and Elachi, C. 1990. F.T. Ulaby and C Elachi, Eds, *Radar polarimetry for geoscience applications*. Artech House.